Commun Nonlinear Sci Numer Simulat 150 (2025) 108978

Contents lists available at ScienceDirect

Communications in Nonlinear Science and Numerical Simulation

journal homepage: www.elsevier.com/locate/cnsns

Research paper

A double inertial embedded modified S-iteration algorithm for nonexpansive mappings: A classification approach for lung cancer detection

Watcharaporn Yajai [a], Kunrada Kankam [b], Jen-Chih Yao [c,d], Watcharaporn Cholamjiak [a,*]

[a] Department of Mathematics, School of Science, University of Phayao, Phayao 56000, Thailand
[b] Elementary Education Program, Faculty of Education, Suan Dusit University Lampang Center, Lampang 52100, Thailand
[c] Center for General Education, China Medical University, Taichung 40402, Taiwan
[d] Academy of Romanian Scientists, Bucharest, Romania

ARTICLE INFO

Dataset link: https://www.kaggle.com/datasets/mysarahmadbhat/lung-cancer

Keywords:
Fixed point problem
Split equilibrium problem
Double inertial technique
Mann algorithm
Classification
Lung cancer

ABSTRACT

This paper introduces a double inertial embedded modified S-iteration algorithm for finding a common fixed point of nonexpansive mappings in a real Hilbert space. A weak convergence theorem is established under suitable conditions involving control parameters. Three algorithms are directly obtained for addressing split equilibrium problems through the equivalence of nonexpansive mappings. An illustrative example in an infinite-dimensional space is provided to substantiate the proposed main algorithm. Furthermore, we highlight the practical application of these algorithms in lung cancer screening, where they are employed to optimize three different machine learning models, thereby potentially improving patient outcomes. The efficiency of the proposed algorithms is validated through comparative analysis with existing algorithms.

1. Introduction

Let H, H_1, and H_2 be real Hilbert spaces, let P, and Q be nonempty closed and convex subsets of the real Hilbert spaces H_1 and H_2, respectively. A mapping $T : \mathsf{H} \to \mathsf{H}$ is nonexpansive if $\|Ta - Tb\| \leq \|a - b\|$ for all $a, b \in \mathsf{H}$. The fixed point problem can be formulated as:

$$\text{finding } \ell^* \in \mathsf{H} \text{ such that } T\ell^* = \ell^*.$$

$F(T)$ is the set of all fixed points of T, that is $F(T) = \{\ell^* \in \mathsf{H} : T\ell^* = \ell^*\}$. The significance of fixed point theorems lies in their ability to guarantee the existence of solutions for various mathematical models, including differential equations and optimization problems, thus serving as essential tools in the analysis of dynamical systems. The fixed point problems in Hilbert spaces involve applying fixed point theory to solve issues related to nonexpansive mappings and convergence to common fixed points. Mann's algorithm [1] employs a linear iteration process where each step's calculations are adjusted to converge to a fixed point. Mann's algorithm is widely used in research involving complex mathematical problems, such as differential equations, partial differential equations, and optimization problems. It is instrumental in computations requiring stability and rapid convergence. Ishikawa's algorithm [2] improves upon Mann's algorithm by utilizing a two-step iteration method, which enhances convergence efficiency to a fixed point.

* Corresponding author.
E-mail addresses: watcharaporn.yajai@gmail.com (W. Yajai), kunrada_kan@dusit.ac.th (K. Kankam), yaojc@mail.cmu.edu.tw (J.-C. Yao), watcharaporn.ch@up.ac.th (W. Cholamjiak).

https://doi.org/10.1016/j.cnsns.2025.108978
Received 16 September 2024; Received in revised form 28 November 2024; Accepted 19 May 2025
Available online 28 May 2025
1007-5704/

This method is suitable for solving problems requiring high-precision numerical computations, such as financial modeling, statistical data analysis, and complex signal processing.

In 1953, Mann [1] introduced the following iterative procedure to approximate a fixed point of a nonexpansive mapping T in a Hilbert space H which generates a sequence as follows: $b^1 \in \mathsf{P}$ and

$$b^{k+1} = \alpha^k b^k + (1-\alpha^k)Tb^k$$

for each $k \in \mathbb{N}$, where $\{\alpha^k\}$ is a real sequence on $[0,1]$. The Mann iteration method has been extensively investigated for approximating fixed points of nonexpansive mappings (see, e.g., [3]). In 2011, Sahu [4] introduced the S-iteration process, where $\{\alpha^k\}, \{\beta^k\} \subset [0,1]$ such that $\alpha \le \alpha^k \le 1$ and $\beta \le \beta^k \le 1$ as follows:

$$\begin{cases} a^0, \in \mathsf{H} \\ b^k = (1-\alpha^k)a^k + \alpha^k T a^k, \\ a^{k+1} = (1-\beta^k)Ta^k + \beta^k T b^k. \end{cases}$$

In 2008, Mainge [5] first introduced the inertial Mann algorithm for a countable family of nonexpansive mappings $\{T^k\}$ by unifying it as follows: He demonstrated that the iterative sequence $\{a^k\}$ converges weakly to a common fixed point in $\cap_{k\ge 1} F(T^k)$ as follows:

$$\begin{cases} a^0, a^1 \in \mathsf{H} \\ b^k = a^k + \theta^k(a^k - a^{k-1}), \\ a^{k+1} = \alpha^k b^k + (1-\alpha^k)T^k b^k. \end{cases}$$

where $\{\alpha^k\}, \{\theta^k\} \subset [0,1]$, and $\theta^k \in [0,\theta]$ for any $\theta \in [0,1]$. Moreover, we study the equilibrium problem (EP) by Ky Fan [6] which is finding a point $\ell^* \in \mathsf{P}$ such that

$$\mathsf{f}^1(\ell^*, v) \ge 0, \ \forall v \in \mathsf{P}. \tag{1.1}$$

The set of solution (1.1) is defined by $EP(\mathsf{f}^1)$. The EP is generalized by several problems such as: variational inequality problem, saddle point problems, Nash–Cournot oligopolistic equilibrium models in economy. Next, the split equilibrium problem (SEP) which was proposed by Moudafi [7] as follows:

$$\begin{aligned} &\text{find } \ell^* \in \mathsf{P} \text{ such that } \mathsf{f}^1(\ell^*, v) \geqslant 0, \ \forall v \in \mathsf{P}, \\ &\text{and } \chi^* = \mathsf{A}\ell^* \in \mathsf{Q} \text{ solves } \mathsf{f}^2(\chi^*, s) \geqslant 0, \ \forall s \in \mathsf{Q} \end{aligned}$$

where $\mathsf{A} : \mathsf{H}_1 \to \mathsf{H}_2$ is a bounded linear operator, let $\mathsf{f}(\cdot,\cdot) : \mathsf{H}\times\mathsf{H} \to \mathbb{R}$ be bifunction where $\mathbb{R}$ is the set of real numbers. Denote $\mathsf{f}^1 : \mathsf{P}\times\mathsf{P} \to \mathbb{R}$ and $\mathsf{f}^2 : \mathsf{Q}\times\mathsf{Q} \to \mathbb{R}$ are bifunctions. Split equilibrium problems extend the utility of fixed point problems by addressing scenarios that involve multiple interdependent systems, offering a robust framework for handling complex, real-world situations that require the simultaneous satisfaction of several criteria [8,9]. These problems are instrumental in developing algorithms that find applications in diverse fields such as signal processing, image reconstruction, resource allocation, network design, and machine learning [10,11].

In 2013, Kazmi and Rizvi [12] proposed an algorithm to find a common solution for the fixed point problem for nonexpansive mapping and the SEP as follows:

$$\begin{cases} b^k = T^{\mathsf{f}^1}_{r^k}(a^k - \beta \mathsf{A}^\top (I - T^{\mathsf{f}^2}_{r^k})\mathsf{A}a^k), \\ c^k = P_{\mathsf{P}}(b^k - \lambda^k T b^k), \\ a^{k+1} = \alpha^k u + \varepsilon^k a^k + \gamma^k S c^k, \end{cases}$$

where $\lambda^k \in (0, 2\tau), \beta \in (0, \frac{1}{L}), \{\alpha^k, \varepsilon^k, \gamma^k\} \subset (0,1), S : \mathsf{P} \to \mathsf{P}$ is nonexpansive and $T : \mathsf{P} \to \mathsf{H}_1$ is inverse strongly monotone. In 2016, Suantai et al. [13] modified Mann's algorithm [1] for solving common problems of the SEP and fixed point problem of nonspreading multivalued mapping $T : \mathsf{P} \to K(\mathsf{P})$ as follows:

$$\begin{cases} a^1 \in \mathsf{P}, \ \forall k \ge 1, \\ b^k = T^{\mathsf{f}^1}_{r^k}(I - \beta \mathsf{A}^\top (I - T^{\mathsf{f}^2}_{r^k})\mathsf{A})a^k, \\ a^{k+1} = \gamma^k a^k + (1-\gamma^k)Tb^k, \end{cases}$$

where $\beta \in (0, \frac{1}{\mathsf{L}})$ such that L is the spectral radius of $\mathsf{A}^\top\mathsf{A}$ and $\mathsf{A}^\top$ is the adjoint of A, $\{r^k\} \subset (0,\infty)$, and $\{\gamma^k\} \subset (0,1)$. Weak convergence theorem is also proved under control conditions on $\{r^k\}$ and $\{\gamma^k\}$.

Inspired by the above mentioned work, we introduce a double inertial technique embedded in a modified S-iteration process for common solution fixed-point problem. We apply this algorithm to address the split equilibrium problem and utilize projection onto constrained solution sets. Finally, we show examples in infinite dimension space, apply machine learning applications for lung cancer datasets, and compare them with other existing methods.

2. Preliminaries

In the sequel, we systematically divide the necessary definitions, lemmas and propositions.

Lemma 2.1 ([14]). *Suppose that $\{\alpha^k\}, \{\xi^k\}$ and $\{c^k\}$ are sequences in $[0,+\infty)$ such that $\alpha^{k+1} \leqslant \alpha^k + c^k(\alpha^k - \alpha^{k-1}) + \xi^k,\ \forall k \geqslant 1,\ \sum_{k=1}^{\infty} \xi^k < +\infty$ and there is $c \in \mathbb{R}$ with $0 \leqslant c^k < c < 1,\ \forall k \geqslant 1$.*

Then the following conditions are satisfied:
(i) $\sum[\alpha^k - \alpha^{k-1}]_+ < +\infty$, where $[\Gamma]_+ = \max\{\Gamma, 0\}$;
(ii) there exists $\alpha^* \in [0,\infty)$ such that $\lim_{k\to+\infty} \alpha^k = \alpha^*$.

Lemma 2.2 ([15]). *Let $T : \mathsf{H} \to \mathsf{H}$ be a nonexpansive mapping such that $F(T) \neq \emptyset$. If there exists a sequence $\{\alpha^k\}$ in H such that $\alpha^k \rightharpoonup \alpha^* \in \mathsf{H}$ and $\|\alpha^k - T\alpha^k\| \to 0$, then $\alpha^* \in F(T)$.*

Lemma 2.3 ([16]). *Let P be a nonempty set of H and $\{\alpha^k\}$ be a sequence in H. Assume that the following conditions hold.*
(i) For every $\alpha^* \in \mathsf{P}$, the sequence $\{\|\alpha^k - \alpha^*\|\}$ converges.
(ii) Every weak sequential cluster point of $\{\alpha^k\}$ belongs to P.
Then $\{\alpha^k\}$ weakly converges to a point in P.

Assumption 2.4 ([17]). Let $\mathsf{f}^1 : \mathsf{P}\times\mathsf{P} \to \mathbb{R}$ be a bifunction satisfying the following assumptions:
(A1) $\mathsf{f}^1(\beta,\beta) = 0$, for all $\beta \in \mathsf{P}$;
(A2) f^1 is monotone, i.e., $\mathsf{f}^1(\beta,\upsilon) + \mathsf{f}^1(\upsilon,\beta) \le 0$ for all $\beta,\upsilon \in \mathsf{P}$;
(A3) for each $\beta,\upsilon,w \in \mathsf{P}$, $\limsup_{c\to0^+} \mathsf{f}^1(cw + (1-c)\beta, \upsilon) \le \mathsf{f}^1(\beta,\upsilon)$;
(A4) for each $\beta \in \mathsf{P}, \upsilon \to \mathsf{f}^1(\beta,\upsilon)$ is convex and lower semi-continuous.

Lemma 2.5 ([18]). *Let $\mathsf{f}^1 : \mathsf{P}\times\mathsf{P} \to \mathbb{R}$ satisfy Assumption 2.4. Denote a mapping $T_r^{\mathsf{f}^1} : \mathsf{H}_1 \to \mathsf{P}$, for each $r > 0$ and $e \in \mathsf{H}_1$, as follows:*

$$T_r^{\mathsf{f}^1}(e) = \{\xi \in \mathsf{P} : \mathsf{f}^1(\xi,\nu) + \frac{1}{r}\langle \nu - \xi, \xi - e\rangle \geqslant 0,\ \forall \nu \in \mathsf{P}\}.$$

Then the following hold:
(1) $T_r^{\mathsf{f}^1}$ is nonempty and single-valued;
(2) $T_r^{\mathsf{f}^1}$ is firmly nonexpansive, i.e., for any $\nu,\xi \in \mathsf{H}_1$,

$$\|T_r^{\mathsf{f}^1}\nu - T_r^{\mathsf{f}^1}\xi\|^2 \le \langle T_r^{\mathsf{f}^1}\nu - T_r^{\mathsf{f}^1}\xi, \nu - \xi\rangle;$$

(3) $EP(\mathsf{f}^1,\mathsf{P}) = F(T_r^{\mathsf{f}^1})$;
(4) $EP(\mathsf{f}^1,\mathsf{P})$ is convex and closed.

Further, let Q be a nonempty closed convex subset of a Hilbert space H_2, and let $\mathsf{f}^2 : \mathsf{Q}\times\mathsf{Q} \to \mathbb{R}$ satisfy Assumption 2.4. Define a mapping $T_s^{\mathsf{f}^2} : \mathsf{H}_2 \to \mathsf{Q}$, for each $s > 0$ and $b \in \mathsf{H}_2$, as follows:

$$T_s^{\mathsf{f}^2}(b) = \{\varrho \in \mathsf{Q} : \mathsf{f}^2(\varrho,\alpha) + \frac{1}{s}\langle \alpha - \varrho, \varrho - b\rangle \geqslant 0,\ \forall \alpha \in \mathsf{Q}\}.$$

Then we easily observe that:
(1) $T_s^{\mathsf{f}^2}$ is nonempty and single-valued;
(2) $T_s^{\mathsf{f}^2}$ is firmly nonexpansive;
(3) $F(T_s^{\mathsf{f}^2}) = EP(\mathsf{f}^2,\mathsf{Q})$;
(4) $EP(\mathsf{f}^2,\mathsf{Q})$ is closed and convex.

3. Main results

In this sequel, we introduce a new two steps inertial technique for the fixed points of two nonexpansive mappings. Throughout the paper, let P be a nonempty closed and convex subset of a real Hilbert space H. Let $T_1, T_2 : \mathsf{H} \to \mathsf{H}$ be nonexpansive mappings such that $F(T_1) \cap F(T_2) \neq \emptyset$.

Algorithm 3.1. Double Inertial Embedded Modified S-Iteration Algorithm

---

Initialization. Select $a^0, b^0, b^{-1} \in \mathsf{H}$, $\{\alpha^k\}, \{\sigma^k\} \subset (0,1)$, $\{\theta^k\}, \{\delta^k\} \subset (-\infty,\infty)$, and $k = 0$.
Step 1. Compute

$$b^{k+1} = (1-\alpha^k)a^k + \alpha^k T_1 a^k.$$

Step 2. Compute

$$c^{k+1} = b^{k+1} + \theta^k(b^{k+1} - b^k) + \delta^k(b^k - b^{k-1}).$$

Step 3. Compute

$$a^{k+1} = (1-\sigma^k)T_1 c^{k+1} + \sigma^k T_2 c^{k+1}.$$

Replace k by $k+1$ and return to **Step 1.**

Theorem 3.2. *Let the sequence $\{a^k\}$ be generated by Algorithm 3.1. Assume that the following conditions hold:*

(i) $\sum_{k=1}^{\infty} |\theta^k| \|b^{k+1} - b^k\| < \infty,\ \sum_{k=1}^{\infty} |\delta^k| \|b^k - b^{k-1}\| < \infty;$

(ii) $0 < \liminf_{k\to\infty} \alpha^k \le \limsup_{k\to\infty} \alpha^k < 1;$

(iii) $0 < \liminf_{k\to\infty} \sigma^k \le \limsup_{k\to\infty} \sigma^k < 1.$

Then, $\{a^k\}$ converges weakly to an element in $F(T_1) \cap F(T_2)$.

Proof. Let $d \in F(T_1) \cap F(T_2)$. By the nonexpansiveness of T_1 and T_2, we have

$$\begin{aligned}
\|a^{k+1} - d\| &= \|(1-\sigma^k)T_1 c^{k+1} + \sigma^k T_2 c^{k+1} - d\| \\
&\le (1-\sigma^k)\|T_1 c^{k+1} - d\| + \sigma^k \|T_2 c^{k+1} - d\| \\
&\le \|c^{k+1} - d\| \\
&\le \|b^{k+1} - d\| + |\theta^k| \|b^{k+1} - b^k\| + |\delta^k| \|b^k - b^{k-1}\| \\
&\le (1-\alpha^k)\|a^k - d\| + \alpha^k \|T_1 a^k - d\| + |\theta^k| \|b^{k+1} - b^k\| + |\delta^k| \|b^k - b^{k-1}\| \\
&\le \|a^k - d\| + |\theta^k| \|b^{k+1} - b^k\| + |\delta^k| \|b^k - b^{k-1}\|.
\end{aligned}$$

By our conditions, it follows from Lemma 2.1 that $\lim_{k\to\infty} \|a^k - d\|$ exists. This implies that $\{a^k\}$ is bounded and $\{b^k\}$ is also bounded. On the other hand, we have

$$\begin{aligned}
\|a^{k+1} - d\|^2 &= (1-\sigma^k)\|T_1 c^{k+1} - d\|^2 + \sigma^k \|T_2 c^{k+1} - d\|^2 - (1-\sigma^k)\sigma^k \|T_1 c^{k+1} - T_2 c^{k+1}\|^2 \\
&\le \|c^{k+1} - d\|^2 - (1-\sigma^k)\sigma^k \|T_1 c^{k+1} - T_2 c^{k+1}\|^2 \\
&\le \|b^{k+1} - d\|^2 + 2\langle \theta^k (b^{k+1} - b^k) + \delta^k (b^k - b^{k-1}), c^{k+1} - d\rangle \\
&\quad - (1-\sigma^k)\sigma^k \|T_1 c^{k+1} - T_2 c^{k+1}\|^2 \\
&= (1-\alpha^k)\|a^k - d\|^2 - \alpha^k \|T_1 a^k - d\|^2 - (1-\alpha^k)\alpha^k \|T_1 a^k - a^k\|^2 \\
&\quad - (1-\sigma^k)\sigma^k \|T_1 c^{k+1} - T_2 c^{k+1}\|^2 + 2\langle \theta^k (b^{k+1} - b^k) + \delta^k (b^k - b^{k-1}), c^{k+1} - d\rangle \\
&\le \|a^k - d\|^2 + 2\langle \theta^k (b^{k+1} - b^k) + \delta^k (b^k - b^{k-1}), c^{k+1} - d\rangle \\
&\quad - (1-\alpha^k)\alpha^k \|T_1 a^k - a^k\|^2 - (1-\sigma^k)\sigma^k \|T_1 c^{k+1} - T_2 c^{k+1}\|^2.
\end{aligned}$$

This implies that

$$\begin{aligned}
&(1-\alpha^k)\alpha^k \|T_1 a^k - a^k\|^2 + (1-\sigma^k)\sigma^k \|T_1 c^{k+1} - T_2 c^{k+1}\|^2 \\
&\qquad \le \|a^k - d\|^2 - \|a^{k+1} - d\|^2 + 2\langle \theta^k (b^{k+1} - b^k) + \delta^k (b^k - b^{k-1}), c^{k+1} - d\rangle.
\end{aligned} \tag{3.1}$$

Since $\lim_{k\to\infty} \|a^k - d\|$ exists, by conditions (i)-(iii) and (3.1), we obtain

$$\lim_{k\to\infty} \|T_1 a^k - a^k\| = \lim_{k\to\infty} \|T_1 c^{k+1} - T_2 c^{k+1}\| = 0. \tag{3.2}$$

By definition of $\{b^k\}$, we have

$$\lim_{k\to\infty} \|b^{k+1} - a^k\| = \lim_{k\to\infty} \alpha^k \|T_1 a^k - a^k\| = 0. \tag{3.3}$$

By the definition of $\{c^k\}$, we have

$$\lim_{k\to\infty} \|c^{k+1} - b^{k+1}\| \le \lim_{k\to\infty} (|\theta^k| \|b^{k+1} - b^k\| + |\delta^k| \|b^k - b^{k-1}\|) = 0. \tag{3.4}$$

It follow from (3.3) and (3.4) that

$$\lim_{k\to\infty} \|c^{k+1} - a^k\| = 0. \tag{3.5}$$

We have,

$$\begin{aligned}
\|a^{k+1} - T_1 c^{k+1}\| &= \|(1-\sigma^k)T_1 c^{k+1} + \sigma^k T_2 c^{k+1} - T_1 c^{k+1}\| \\
&\le |\sigma^k| \|T_1 c^{k+1} - T_2 c^{k+1}\|.
\end{aligned}$$

From Eq. (3.2), we obtain that

$$\lim_{k\to\infty} \|a^{k+1} - T_1 c^{k+1}\| = 0. \tag{3.6}$$

Using (3.2), (3.5), and (3.6), we have

$$\begin{aligned}\|a^{k+1} - a^k\| &\le \|a^{k+1} - T_1 c^{k+1}\| + \|T_1 c^{k+1} - T_1 a^k\| + \|T_1 a^k - a^k\| \\ &\le \|a^{k+1} - T_1 c^{k+1}\| + \|c^{k+1} - a^k\| + \|T_1 a^k - a^k\|.\end{aligned}$$

We get that

$$\lim_{k\to\infty} \|a^{k+1} - a^k\| = 0. \tag{3.7}$$

Then, using (3.2), (3.5), (3.6) and (3.7), we have

$$\|T_2 c^{k+1} - c^{k+1}\| \le \|T_2 c^{k+1} - T_1 c^{k+1}\| + \|T_1 c^{k+1} - a^{k+1}\| + \|a^{k+1} - a^k\| + \|a^k - c^{k+1}\|,$$

from which it follows that

$$\lim_{k\to\infty} \|T_2 c^{k+1} - c^{k+1}\| = 0. \tag{3.8}$$

Since $\{a^k\}$ is bounded, we suppose that a^* is a weak sequential cluster point of a^k. It follow from (3.5) that a^* is also a weak sequential cluster point of c^{k+1}. By using Lemma 2.2 with (3.2), and (3.8), we can get that $a^* \in F(T_1) \cap F(T_2)$. By applying Opial's Lemma 2.3, we obtain that $\{a^k\}$ converges weakly to an element in $F(T_1) \cap F(T_2)$. □

Denote $\mathbb{E}$ to be a nonempty closed convex subset of H. Assume that $\mathsf{A} : \mathsf{H}_1 \to \mathsf{H}_2$ is a bounded linear operator. Let $\mathsf{f}^1 : \mathsf{P} \times \mathsf{P} \to \mathbb{R}$, $\mathsf{f}^2 : \mathsf{Q} \times \mathsf{Q} \to \mathbb{R}$ be two bifunctions satisfying Assumption 2.4 and f^2 is upper semi-continuous in the first argument. Let L be the spectral radius of $\mathsf{A}^\mathsf{T}\mathsf{A}$ and A^T is the adjoint of A with $\xi = \{\ell^* \in EP(\mathsf{f}^1)$ and $\mathsf{A}\ell^* \in EP(\mathsf{f}^2)\}$. To apply our Algorithm 3.1 to solve split equilibrium problem, we use $T_r^{\mathsf{f}^1}(I - \beta \mathsf{A}^\mathsf{T}(I - T_r^{\mathsf{f}^2})\mathsf{A})$ which is nonexpansive when $\beta \in (0, \frac{1}{\mathsf{L}}]$, as demonstrated in the proof of Byrne [19], and $P_{\mathbb{E}}$ is nonexpansive as discussed by Combettes [20]. Based on these parameters, we derive the following three algorithms:

Algorithm 3.3. Double Inertial Embedded Two-Steps Split Equilibrium Algorithm

Initialization. Select $a^0, b^0, b^{-1} \in \mathsf{H}$, $\{\alpha^k\}, \{\sigma^k\} \subset (0,1)$, $\{\theta^k\}, \{\delta^k\} \subset (-\infty, \infty)$, $r \subset (0,\infty)$, $\beta \in (0, \frac{1}{\mathsf{L}})$, and $k = 0$.

Step 1. Compute

$$b^{k+1} = (1-\alpha^k)a^k + \alpha^k T_r^{\mathsf{f}^1}(I - \beta \mathsf{A}^\mathsf{T}(I - T_r^{\mathsf{f}^2})\mathsf{A})a^k.$$

Step 2. Compute

$$c^{k+1} = b^{k+1} + \theta^k(b^{k+1} - b^k) + \delta^k(b^k - b^{k-1}).$$

Step 3. Compute

$$a^{k+1} = (1-\sigma^k)T_r^{\mathsf{f}^1}(I - \beta \mathsf{A}^\mathsf{T}(I - T_r^{\mathsf{f}^2})\mathsf{A})c^{k+1} + \sigma^k T_r^{\mathsf{f}^1}(I - \beta \mathsf{A}^\mathsf{T}(I - T_r^{\mathsf{f}^2})\mathsf{A})c^{k+1}.$$

Replace k by $k+1$ and return to **Step 1.**

Algorithm 3.4. Double Inertial Embedded Two-Steps Projective Split Equilibrium Algorithm I

Initialization. Select $a^0, b^0, b^{-1} \in \mathsf{H}$, $\{\alpha^k\}, \{\sigma^k\} \subset (0,1)$, $\{\theta^k\}, \{\delta^k\} \subset (-\infty, \infty)$, $r \subset (0,\infty)$, $\beta \in (0, \frac{1}{\mathsf{L}})$, and $k = 0$.

Step 1. Compute

$$b^{k+1} = (1-\alpha^k)a^k + \alpha^k T_r^{\mathsf{f}^1}(I - \beta \mathsf{A}^\mathsf{T}(I - T_r^{\mathsf{f}^2})\mathsf{A})a^k.$$

Step 2. Compute

$$c^{k+1} = b^{k+1} + \theta^k(b^{k+1} - b^k) + \delta^k(b^k - b^{k-1}).$$

Step 3. Compute

$$a^{k+1} = (1-\sigma^k)T_r^{\mathsf{f}^1}(I - \beta \mathsf{A}^\mathsf{T}(I - T_r^{\mathsf{f}^2})\mathsf{A})c^{k+1} + \sigma^k P_{\mathbb{E}} c^{k+1}.$$

Replace k by $k+1$ and return to **Step 1.**

Algorithm 3.5. Double Inertial Embedded Two-Steps Projective Split Equilibrium Algorithm II

Initialization. Select $a^0, b^0, b^{-1} \in \mathsf{H}$, $\{\alpha^k\}, \{\sigma^k\} \subset (0,1)$, $\{\theta^k\}, \{\delta^k\} \subset (-\infty, \infty)$, $r \subset (0,\infty)$, $\beta \in (0, \frac{1}{\mathsf{L}})$, and $k = 0$.
Step 1. Compute

$$b^{k+1} = (1-\alpha^k)a^k + \alpha^k P_{\mathbb{E}} a^k.$$

Step 2. Compute

$$c^{k+1} = b^{k+1} + \theta^k(b^{k+1} - b^k) + \delta^k(b^k - b^{k-1}).$$

Step 3. Compute

$$a^{k+1} = (1-\sigma^k)P_{\mathbb{E}} c^{k+1} + \sigma^k T_r^{f^1}(I - \beta \mathsf{A}^\top (I - T_r^{f^2})\mathsf{A})c^{k+1}.$$

Replace k by $k+1$ and return to **Step 1.**

Theorem 3.6. *Let $\{a^k\}$ be the sequence generated by Algorithms 3.3–3.5. Assume that the conditions (i)–(iii) in Theorem 3.2 hold. Then, $\{a^k\}$ converges weakly to an element in ξ.*

Proof. It suffices to demonstrate only if $a^* \in F(T_r^{f^1}(I - \beta\mathsf{A}^\top(I - T_r^{f^2})\mathsf{A}))$, then $a^* \in \xi$. Let $\rho \in \xi$ and $a^* = T_r^{f^1}(I - \beta\mathsf{A}^\top(I - T_r^{f^2})\mathsf{A})a^*$. Then, we have

$$\begin{aligned}
\|a^* - \rho\|^2 &= \|T_r^{f^1}(I - \beta\mathsf{A}^\top(I - T_r^{f^2})\mathsf{A})a^* - \rho\|^2 \\
&= \|T_r^{f^1}(I - \beta\mathsf{A}^\top(I - T_r^{f^2})\mathsf{A})a^* - T_r^{f^1}\rho\|^2 \\
&\le \|a^* - \beta\mathsf{A}^\top(I - T_r^{f^2})\mathsf{A}a^* - \rho\|^2 \\
&\le \|a^* - \rho\|^2 + \beta^2\|\mathsf{A}^\top(I - T_r^{f^2})\mathsf{A}a^*\|^2 + 2\beta\langle \rho - a^*, \mathsf{A}^\top(I - T_r^{f^2})\mathsf{A}a^*\rangle. \\
&= \|a^* - \rho\|^2 + \beta^2\langle \mathsf{A}a^* - T_r^{f^2}\mathsf{A}a^*, \mathsf{A}\mathsf{A}^\top(I - T_r^{f^2})\mathsf{A}a^*\rangle \\
&\quad + 2\beta\langle \rho - a^*, \mathsf{A}^\top(I - T_r^{f^2})\mathsf{A}a^*\rangle.
\end{aligned} \tag{3.9}$$

On the other hand, we have

$$\begin{aligned}
\beta^2\langle \mathsf{A}a^* - T_r^{f^2}\mathsf{A}a^*, \mathsf{A}\mathsf{A}^\top(I - T_r^{f^2})\mathsf{A}a^*\rangle &\le \mathsf{L}\beta^2\langle \mathsf{A}a^* - T_r^{f^2}\mathsf{A}a^*, \mathsf{A}a^* - T_r^{f^2}\mathsf{A}a^*\rangle \\
&= \mathsf{L}\beta^2\|\mathsf{A}a^* - T_r^{f^2}\mathsf{A}a^*\|^2
\end{aligned} \tag{3.10}$$

and

$$\begin{aligned}
2\beta\langle \rho - a^*, \mathsf{A}^\top(I - T_r^{f^2})\mathsf{A}a^*\rangle &= 2\beta\langle \mathsf{A}(\rho - a^*), \mathsf{A}a^* - T_r^{f^2}\mathsf{A}a^*\rangle \\
&= 2\beta\langle \mathsf{A}(\rho - a^*) + (\mathsf{A}a^* - T_r^{f^2}\mathsf{A}a^*) \\
&\quad - (\mathsf{A}a^* - T_r^{f^2}\mathsf{A}a^*), \mathsf{A}a^* - T_r^{f^2}\mathsf{A}a^*\rangle \\
&= 2\beta\{\langle \mathsf{A}\rho - T_r^{f^2}\mathsf{A}a^*, \mathsf{A}a^* - T_r^{f^2}\mathsf{A}a^*\rangle - \|\mathsf{A}a^* - T_r^{f^2}\mathsf{A}a^*\|^2\} \\
&\le 2\beta\{\frac{1}{2}\|\mathsf{A}a^* - T_r^{f^2}\mathsf{A}a^*\|^2 - \|\mathsf{A}a^* - T_r^{f^2}\mathsf{A}a^*\|^2\} \\
&= -\beta\|\mathsf{A}a^* - T_r^{f^2}\mathsf{A}a^*\|^2.
\end{aligned} \tag{3.11}$$

Using (3.9), (3.10), and (3.11), we have

$$\begin{aligned}
\|a^* - \rho\|^2 &\le \|a^* - \rho\|^2 + \mathsf{L}\beta^2\|\mathsf{A}a^* - T_r^{f^2}\mathsf{A}a^*\|^2 - \beta\|\mathsf{A}a^* - T_r^{f^2}\mathsf{A}a^*\|^2 \\
&= \|a^* - \rho\|^2 + \beta(\mathsf{L}\beta - 1)\|\mathsf{A}a^* - T_r^{f^2}\mathsf{A}a^*\|^2.
\end{aligned} \tag{3.12}$$

Since $\beta \in (0, \frac{1}{\mathsf{L}})$, it follows from (3.12) that $\|\mathsf{A}a^* - T_r^{f^2}\mathsf{A}a^*\| = 0$. This implies that $\mathsf{A}a^* = T_r^{f^2}\mathsf{A}a^*$. Therefore, $a^* = T_r^{f^1}a^* = T_r^{f^1}(a^* - \beta\mathsf{A}^\top(0)) = T_r^{f^1}(I - \beta\mathsf{A}^\top(I - T_r^{f^2})\mathsf{A})a^*$. □

For supporting our main theorem, we now give an example in infinitely dimensional spaces $L_2[0,1]$ such that $\|.\|$ is L_2-norm defined by $\|x\| = \sqrt{\int_0^1 |x(t)|^2 dt}$ where $x(t) \in L_2[0,1]$.

Example 3.7. Let $\mathsf{H} = L_2[0,1]$, $T_1, T_2 : \mathsf{H} \to \mathsf{H}$ be defined by $T_1 a(t) = \frac{2}{3}a(t)$, $T_2 a(t) = \frac{1}{2}a(t)$, for all $a(t) \in L_2[0,1]$.

Next, we set parameter for each algorithm see in Table 1.

We consider for comparison in 4 cases, with different T and initialization. We use the Cauchy error $\|a^k - a^{k-1}\|^2 < 10^{-3}$ for the stopping criterion. We set all of the parameters for Algorithm 3.1 and algorithm in literature seen in Table 1.

Case 1: We set $T_1 a(t) = \frac{2}{3}a(t)$ and $a_1 = sin(t) - 2$, $b_0 = t^2$ and $b_1 = t^2 - 1$ (see Fig. 1 on the left).

Table 1
Setting every parameter.

	α^k	θ^k	δ^k	σ^k
Algorithm 3.1	0.9	$\frac{1}{k^2+1}$	$\frac{1}{k^2+10}$	0.9
Algorithm of Mainge [5]	0.9	$\frac{1}{k^2+1}$	–	–

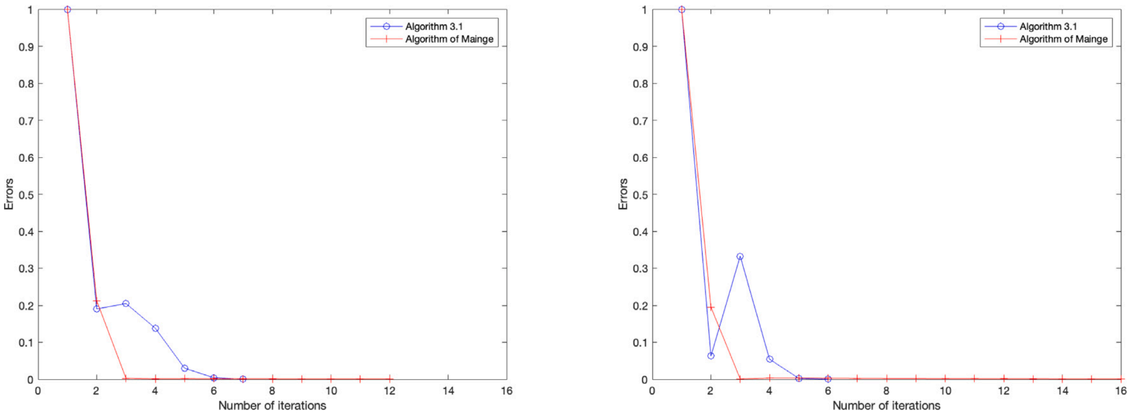

Fig. 1. On the left is the Cauchy error plotting of Algorithm 3.1 and Algorithm of Mainge [5] in Case 1 and on the right is the Cauchy error plotting of Algorithm 3.1 and Algorithm of Mainge [5] in Case 2.

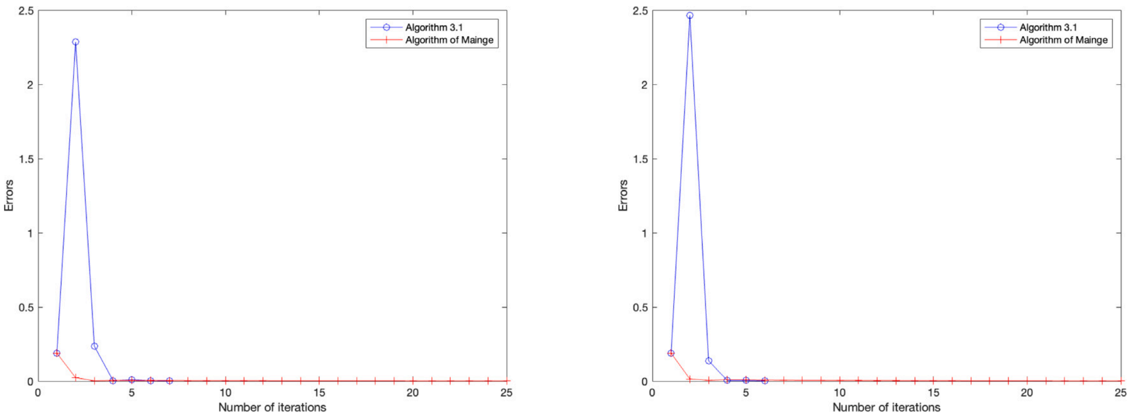

Fig. 2. On the left is the Cauchy error plotting of Algorithm 3.1 and Algorithm of Mainge [5] in Case 3 and on the right is the Cauchy error plotting of Algorithm 3.1 and Algorithm of Mainge [5] in Case 4.

Case 2: We set $T_2 a(t) = \frac{1}{2} a(t)$ and $a_1 = sin(t) - 2, b_0 = t^2$ and $b_1 = t^2 - 1$ (see Fig. 1 on the right).
Case 3: We set $T_1 a(t) = \frac{2}{3} a(t)$ and $a_1 = t^2, b_0 = t^2 + 1$ and $b_1 = e^t$ (see Fig. 2 on the left).
Case 4: We set $T_2 a(t) = \frac{1}{2} a(t)$ and $a_1 = t^2, b_0 = t^2 + 1$ and $b_1 = e^t$ (see Fig. 2 on tghe right).

4. Application to data classification problem

Lung cancer is a malignant condition characterized by uncontrolled cell growth in the lung tissues. It is one of the most common and deadliest forms of cancer worldwide, largely due to smoking, which accounts for about 85% of all cases. There are two primary types: non-small cell lung cancer (NSCLC), which comprises approximately 85% of cases, and small cell lung cancer (SCLC), which is more aggressive but less common. Symptoms often include persistent cough, chest pain, and difficulty breathing, but they typically appear only in advanced stages, making early detection challenging. Risk factors extend beyond smoking to include exposure to radon gas, asbestos, and family history of the disease. Diagnosis is usually confirmed through imaging tests like CT scans and tissue biopsy. Treatment options depend on the cancer type and stage, ranging from surgery and radiation to chemotherapy and targeted therapies. Early detection and advances in treatment are crucial for improving survival rates. The application of mathematical algorithms like ELMs in lung cancer prediction offers numerous benefits, including early detection, improved diagnostic accuracy, personalized treatment plans, cost efficiency, and real-time analysis. These tools enhance the ability of healthcare providers to offer

Table 2
Summary statistics.

	Min	Max	Mean	Median	Mode	Std	Variance
Gender	1	2	1.5243	2	2	0.5002	0.2502
Age	21	87	62.6731	62	64	8.2103	67.4090
Smoking	1	2	1.5631	2	2	0.4968	0.2468
Yellow fingers	1	2	1.5696	2	2	0.4959	0.2460
Anxiety	1	2	1.4984	1	1	0.5008	0.2508
Peer pressure	1	2	1.5016	2	2	0.5008	0.2508
Chronic disease	1	2	1.5049	2	2	0.5008	0.2508
Fatigue	1	2	1.6731	2	2	0.4698	0.2207
Allergy	1	2	1.5566	2	2	0.4976	0.2476
Wheezing	1	2	1.5566	2	2	0.4976	0.2476
Alcohol consuming	1	2	1.5566	2	2	0.4976	0.2476
Coughing	1	2	1.5793	2	2	0.4945	0.2445
Shortness of breath	1	2	1.6408	2	2	0.4806	0.2309
Swallowing difficulty	1	2	1.4693	1	1	0.4999	0.2499
Chest pain	1	2	1.5566	2	2	0.4976	0.2476
Lung cancer	0	1	0.8738	1	1	0.3326	0.1106

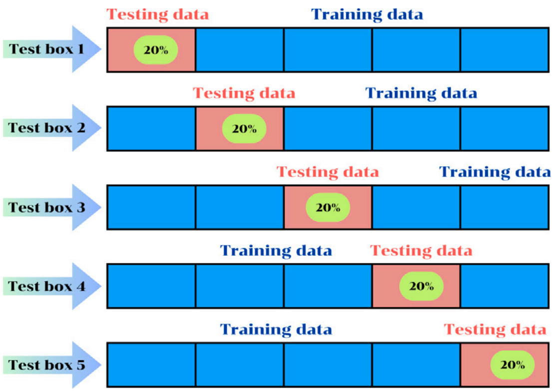

Fig. 3. Training data and testing data.

timely and effective treatment, ultimately improving patient outcomes. The integration of advanced mathematical techniques in medical diagnostics represents a significant advancement in the fight against lung cancer.

In this paper, we use dataset in the Kaggle website (https://www.kaggle.com/datasets/mysarahmadbhat/lung-cancer), which have 1 target and 15 features; gender, age, smoking, yellow fingers, anxiety, peer pressure, chronic disease, fatigue, allergy, whezzing, alcohol, coughing, shortness of breath, swallowing difficulty, and chest pain. For the statistics of lung cancer dataset seen in Table 2.

Table 2 describes every each feature such as Age: Mean value is 62.67 which means the average age of the participants is around 63 years old, Smoking: Mean value is 1.56 that there are slightly more non-smokers than smokers, and Anxiety: Mean value is 1.50 that means equal distribution of people with and without anxiety.

In Fig. 3, we need to divide the data equally for 75% of training data and 25% of testing data. So, we will to calculated 5 boxs. For our applying in machine learning, by Huang et al. [21], we use *Extreme Learning Machine* (ELM). This concept was explained by let $S := \{(\mathbf{s}_n, \mathbf{r}_n) : \mathbf{s}_n \in \mathbb{R}^N, \mathbf{r}_n \in \mathbb{R}^M, n = 1, 2, \dots, P\}$ for being a training set where $\mathbf{s}_n$ is an input training data and $\mathbf{r}_n$ is a training target. For single-hidden layer feed forward neural networks (SLFNs) with D hidden nodes, the output function is in the form

$$\mathbf{Q}_n = \sum_{k=1}^{D} E_k V(c_k \mathbf{s}_n + d_k),$$

where V is activated function, c_k is weight matrix and d_k is vector of finally the bias, and E_k is the optimal output weight at the kth hidden node. To find optimal output weight E_k, the hidden layer output matrix L is defined as follows:

$$L = \begin{bmatrix} V(c_1\mathbf{s}_1 + d_1) & \dots & V(c_D\mathbf{s}_1 + d_D) \\ \vdots & \ddots & \vdots \\ V(c_1\mathbf{s}_P + d_1) & \dots & V(c_D\mathbf{s}_P + d_D) \end{bmatrix}$$

To solve ELM is to find optimal output weight $E = [E_1^T, \dots, E_D^T]^T$ such that $LE = T$, where $T = [\mathbf{r}_1^T, \dots, \mathbf{r}_P^T]^T$ is the training data. In some cases, finding $E = L^{\dagger}T$, where $L^{\dagger}$ is the *Moore–Penrose generalized inverse* of L. We can solve $LE = T$ by the following least square problems

$$\min_{E\in\mathbb{R}^M} \{\|LE - T\|_2^2\}. \tag{4.1}$$

For applying our algorithm to solve (4.1), we set

$$\mathsf{f}^1(\nu,\alpha)=\begin{cases}0, & \forall \nu,\alpha\in \mathsf{P},\\ -1, & otherwise\end{cases} \tag{4.2}$$

$$\mathsf{f}^2(\nu,\alpha)=\begin{cases}0, & \forall \nu,\alpha\in \mathsf{Q},\\ -1, & otherwise\end{cases} \tag{4.3}$$

Then, our algorithm can be reduced to solve the split feasibility problem (SFP) which was introduced by Censor and Elfving [22] as follows: finding a point $\nu^*\in\mathsf{P}$ such that

$$\mathsf{A}\nu^*\in\mathsf{Q} \tag{4.4}$$

where P,Q are nonempty closed and convex subsets of $\mathbb{R}^B$ and $\mathbb{R}^D$, respectively, A is a $B\times D$ real matrix. We create 3 model for our Algorithm 3.3 of the split feasibility problem (4.4) to obtain results in machine learning (4.1).

1. Least square model - (L)

$$\min_{\nu\in\mathsf{H}_1}\frac{1}{2}\|P_{\mathsf{Q}}LE-LE\|_2^2, \tag{4.5}$$

setting $\mathsf{A}=L,\mathsf{Q}=\{T\}$ and $\mathsf{P}=\mathsf{H}_1$.

2. Least square on constraint set L_1 - (LL_1)

$$\min_{\nu\in\mathsf{P}}\frac{1}{2}\|P_{\mathsf{Q}}LE-LE\|_2^2, \tag{4.6}$$

setting $\mathsf{A}=L,\mathsf{Q}=\{T\}$ and $\mathsf{P}=\{\nu\in\mathsf{H}_1:\|\nu\|_1\le\tau\}$ where $\tau>0$.

3. Least square on constraint set L_2 - (LL_2)

$$\min_{\nu\in\mathsf{P}}\frac{1}{2}\|P_{\mathsf{Q}}LE-LE\|_2^2, \tag{4.7}$$

setting $\mathsf{A}=L,\mathsf{Q}=\{T\}$ and $\mathsf{P}=\{\nu\in\mathsf{H}_1:\|\nu\|_2^2\le\tau\}$ where $\tau>0$.

In this research, we utilize the binary cross-entropy loss function, when $\hat z_k$ is the kth scalar value in the model output, z_k is the corresponding target value and W is the number of scalar values in the model output, defined as following:

$$Loss=-\frac{1}{\mathsf{W}}\sum_{k=1}^{\mathsf{W}}z_k\log\hat z_k+(1-z_k)\log(1-\hat z_k).$$

In this paper, Precision defines the potential of positive prediction; Recall defines the model's quality to detect pertinent data and Accuracy denotes the rate of correct predictions by the model. The formulation of 3 measures [23] are denoted as follows:

$$\text{Precision(Pre)}=\frac{TP}{TP+FP}\times100\%. \tag{4.8}$$

$$\text{Recall(Rec)}=\frac{TP}{TP+FN}\times100\%. \tag{4.9}$$

$$\text{Accuracy(Acc)}=\frac{TP+TN}{TP+FP+TN+FN}\times100\%. \tag{4.10}$$

where True Positive (TP) are the elements that have been labeled as positive by the model and they are actually positive, True Negative (TN) are the elements that have been labeled as negative by the model and they are actually negative, False Positives (FP) are the elements that have been labeled as positive by the model, but they are actually negative, and False Negatives (FN) are the elements that have been labeled as negative by the model, but they are actually positive. Likewise, N and P are the Negative, and Positive population of Malignant and Benign cases, respectively. We defines F1-Score to be the harmonic mean value between recall and precision as follows:

$$\text{F1-Score}=2\left(\frac{\text{Precision}\times\text{Recall}}{\text{Precision}+\text{Recall}}\right)\times100\%. \tag{4.11}$$

We set the activation function as sigmoid, hidden nodes $D=400$, regularization parameter $\alpha^k=0.9$, and $\sigma^k=0.9$.

When

$$\theta^k=\begin{cases}\frac{2^{12}}{\|b^k-b^{k-1}\|^5+k^5+2^{12}}, & \text{if } b^k\ne b^{k-1} \text{ and } k>M,\\ \theta, & \text{otherwise}\end{cases}$$

and

$$\delta^k=\begin{cases}\frac{2^{15}}{\|b^k-b^{k-1}\|^2+k^2+2^{15}}, & \text{if } b^k\ne b^{k-1} \text{ and } k>M,\\ \delta, & \text{otherwise.}\end{cases}$$

Setting the Kazmi and Rizvi [12] algorithm as follows:

$$\text{model 1}\begin{cases}b^k=T_{r^k}^{\mathsf{f}^1}(a^k-\beta\mathsf{A}^{\mathsf{T}}(I-T_{r^k}^{\mathsf{f}^2})\mathsf{A}a^k),\\ c^k=P_{\mathsf{P}}(b^k-\lambda^kTb^k),\\ a^{k+1}=\alpha^ku+\varepsilon^ka^k+\gamma^kc^k,\end{cases} \tag{4.12}$$

Table 3
Choose the parameters for every algorithms.

	β	λ^k	α^k	σ^k	θ^k	δ^k	ε^k	γ^k
Algorithm 3.3	$\frac{0.9999}{max(eigenvalue(\mathsf{A}^T\mathsf{A}))}$	–	0.9	0.9	$\frac{2^{12}}{\Vert b^k-b^{k-1}\Vert^5+k^5+2^{12}}$	$\frac{2^{15}}{\Vert b^k-b^{k-1}\Vert^2+k^2+2^{15}}$	–	–
Algorithm 3.4	$\frac{0.9999}{max(eigenvalue(\mathsf{A}^T\mathsf{A}))}$	–	0.9	0.9	$\frac{2^{12}}{\Vert b^k-b^{k-1}\Vert^5+k^5+2^{12}}$	$\frac{2^{15}}{\Vert b^k-b^{k-1}\Vert^2+k^2+2^{15}}$	–	–
Algorithm 3.5	$\frac{0.9999}{max(eigenvalue(\mathsf{A}^T\mathsf{A}))}$	–	0.9	0.9	$\frac{2^{12}}{\Vert b^k-b^{k-1}\Vert^5+k^5+2^{12}}$	$\frac{2^{15}}{\Vert b^k-b^{k-1}\Vert^2+k^2+2^{15}}$	–	–
Algorithm of Kazmi [12] model 1	$\frac{0.9999}{max(eigenvalue(\mathsf{A}^T\mathsf{A}))}$	$\frac{1.9999}{max(eigenvalue(\mathsf{A}^T\mathsf{A}))}$	0.1	–	–	–	0.3	0.6
Algorithm of Kazmi [12] model 2	$\frac{0.9999}{max(eigenvalue(\mathsf{A}^T\mathsf{A}))}$	$\frac{1.9999}{max(eigenvalue(\mathsf{A}^T\mathsf{A}))}$	0.1	–	–	–	0.3	0.6
Algorithm of Suantai [13]	$\frac{0.9999}{max(eigenvalue(\mathsf{A}^T\mathsf{A}))}$	–	–	–	–	–	–	0.9

Table 4
Efficiency comparative of existing algorithms and our algorithms.

Test box 1	Iter	Acc (%)	Pre (%)	Rec (%)	F1 (%)	Time
Algorithm 3.3	55	90.16	90.00	100	94.74	0.3763
Algorithm 3.4	23	90.16	90.00	100	94.74	0.1462
Algorithm 3.5	29	90.16	90.00	100	94.74	0.1219
Algorithm of Kazmi [12] model 1	55	88.52	88.52	100	93.91	0.2922
Algorithm of Kazmi [12] model 2	55	88.52	88.52	100	93.91	0.3982
Algorithm of Suantai [13]	55	88.52	88.52	100	93.91	0.1769
Test box 2						
Algorithm 3.3	47	87.10	87.10	100	93.10	0.3261
Algorithm 3.4	33	87.10	87.10	100	93.10	0.1663
Algorithm 3.5	30	87.10	87.10	100	93.10	0.0711
Algorithm of Kazmi [12] model 1	47	87.10	87.10	100	93.10	0.2913
Algorithm of Kazmi [12] model 2	47	87.10	87.10	100	93.10	0.3298
Algorithm of Suantai [13]	47	87.10	87.10	100	93.10	0.4501
Test box 3						
Algorithm 3.3	150	91.94	91.53	100	95.58	0.8418
Algorithm 3.4	50	95.16	96.36	98.15	97.25	0.2452
Algorithm 3.5	78	95.16	96.36	98.15	97.25	0.2557
Algorithm of Kazmi [12] model 1	150	87.10	87.10	100	93.10	0.8617
Algorithm of Kazmi [12] model 2	150	87.10	87.10	100	93.10	0.8450
Algorithm of Suantai [13]	150	87.10	87.10	100	93.10	0.8479
Test box 4						
Algorithm 3.3	46	87.10	87.10	100	93.10	0.1135
Algorithm 3.4	23	87.10	87.10	100	93.10	0.1671
Algorithm 3.5	34	87.10	87.10	100	93.10	0.1556
Algorithm of Kazmi [12] model 1	46	87.10	87.10	100	93.10	0.2936
Algorithm of Kazmi [12] model 2	46	87.10	87.10	100	93.10	0.3224
Algorithm of Suantai [13]	46	87.10	87.10	100	93.10	0.2550
Test box 5						
Algorithm 3.3	118	93.55	93.10	100	96.43	0.5107
Algorithm 3.4	101	93.55	93.10	100	96.43	0.4332
Algorithm 3.5	102	93.55	93.10	100	96.43	0.2566
Algorithm of Kazmi [12] model 1	118	87.10	87.10	100	93.10	0.6645
Algorithm of Kazmi [12] model 2	118	87.10	87.10	100	93.10	0.6993
Algorithm of Suantai [13]	118	87.10	87.10	100	93.10	0.7008

$$\text{model 2}\begin{cases} b^k = T^{\mathsf{f}^1}_{r^k}(a^k - \beta\mathsf{A}^\top(I - T^{\mathsf{f}^2}_{r^k})\mathsf{A}a^k), \\ c^k = P_{\mathsf{P}}(b^k - \lambda^k T b^k), \\ a^{k+1} = \alpha^k u + \varepsilon^k a^k + \gamma^k T^{\mathsf{f}^1}_{r^k}(I - \gamma\mathsf{A}^\top(I - T^{\mathsf{f}^2}_{r^k})\mathsf{A})c^k. \end{cases} \tag{4.13}$$

We select every parameters seen in Table 3.

Next, we show performance for our algorithms and comparison with previous literature algorithms.

From Table 4, in the test box 1, Algorithms 3.3, 3.4, 3.5 is the best with accuracy 90.16%, precision 90.00%, recall 100% and F1 Score 94.74%. In the test box 2, Algorithms 3.3, 3.4, 3.5 is the best with accuracy 87.10%, precision 87.10%, recall 100% and F1 Score 93.10%. In the test box 3, Algorithms 3.4, 3.5 is the best with accuracy 95.16%, precision 96.36%, recall 98.15% and F1 Score 97.25%. In the test box 4, Algorithms 3.3, 3.4, 3.5 is the best with accuracy 87.10%, precision 87.10%, recall 100% and F1

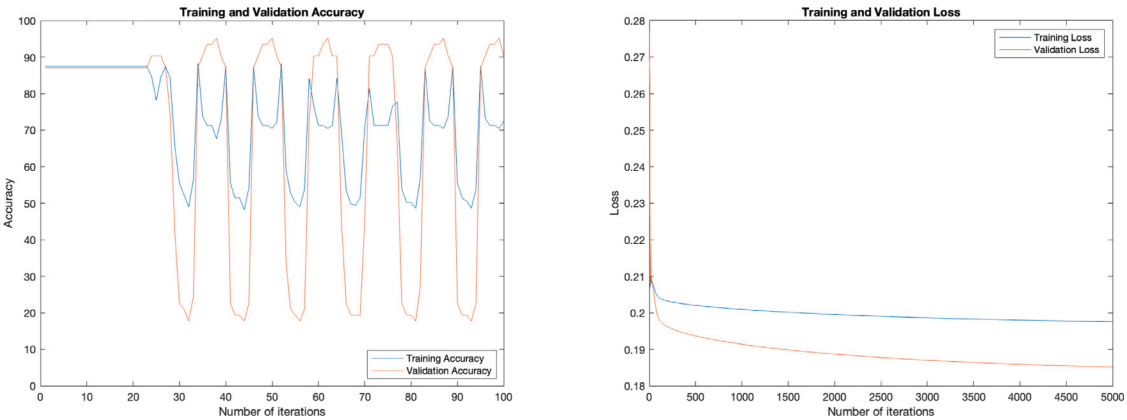

Fig. 4. On the left is the training and validation accuracy of Algorithm 3.4 in test box 3 and on the right is the training and validation loss of Algorithm 3.4 in test box 3.

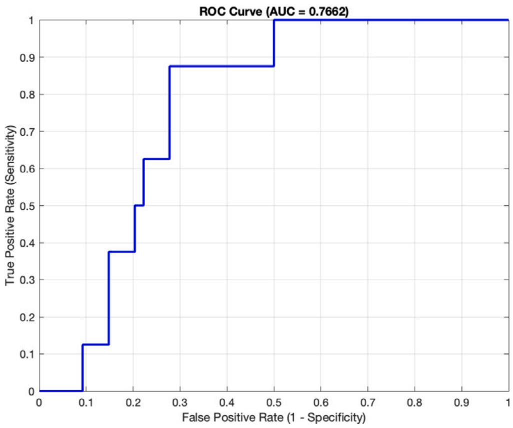

Fig. 5. ROC curve of Algorithm 3.4 in test box 3.

Score 93.10%. In the test box 5, Algorithms 3.3, 3.4, 3.5 is the best with accuracy 93.55%, precision 93.10%, recall 100% and F1 Score 96.43%. The highest accuracy observed was 95.16% in test box 3, achieved by Algorithm 3.4. Algorithm 3.4 stands out as the best overall due to its combination of high performance and faster execution time across different test boxes.

From Fig. 4, we saw that our Algorithm 3.4 has good fit model which means that our Algorithm 3.4 appropriately learns the training dataset and generalizes well to classify the lung cancer dataset (see Fig. 5).

The ROC curve presented, with an AUC (Area Under the Curve) of 0.7662, indicates a moderately effective model for predicting lung cancer. This model demonstrates a reasonable ability to differentiate between positive and negative cases (patients with lung cancer) (patients without the disease). The y-axis represents the true positive rate, which reflects the proportion of actual lung cancer cases correctly identified by the model, while the x-axis represents the false positive rate, indicating the proportion of actual non-cancer cases that are incorrectly classified as positive. An AUC of 0.7662 suggests a fair level of diagnostic accuracy, making the model potentially useful for clinical applications in lung cancer detection. The model could assist in early diagnosis and inform treatment planning, thereby aiding clinicians in making more accurate decisions regarding patient care. Additionally, the ROC curve facilitates the determination of an optimal classification threshold, enhancing the model's clinical applicability by allowing adjustments based on specific diagnostic criteria and the prevalence rates observed in different populations.

5. Conclusion

In this paper, we introduced a double inertial technique aimed at solving the fixed point problem in real Hilbert spaces. Our approach was grounded in the development of a weak convergence theorem for the proposed algorithm, ensuring the theoretical robustness of our method. The practical applicability of our algorithm was demonstrated by its application to the split equilibrium problem. Moreover, in Section 4, we extended the utility of our algorithm by applying it to a real-world problem: the classification of lung cancer data using machine learning. The performance of our algorithm was rigorously evaluated and compared with existing algorithms. The highest accuracy was 95.16% in test box 3, achieved by Algorithm 3.4, marking it as the best overall due to its balance of high performance and efficient execution. This positions our algorithm as a valuable tool in the early and accurate detection of lung cancer, potentially contributing to better patient outcomes and more effective healthcare management.

CRediT authorship contribution statement

Watcharaporn Yajai: Writing – original draft. **Kunrada Kankam:** Writing – review & editing. **Jen-Chih Yao:** Writing – review & editing. **Watcharaporn Cholamjiak:** Writing – review & editing.

Funding

University of Phayao and Thailand Science Research and Innovation Fund (Fundamental Fund 2025, Grant No. 5013/2567).

Declaration of competing interest

The authors declare that they have no known competing financial interests or personal relationships that could have appeared to influence the work reported in this paper.

Acknowledgment

The authors would like to thank the University of Phayao.

Data availability

Data Availability in Kaggle (https://www.kaggle.com/datasets/mysarahmadbhat/lung-cancer).

References

[1] Mann WR. Mean value methods in iteration. Proc Amer Math Soc 1953;4(3):506–10.
[2] Sokhuma K, Kaewkhao A. Ishikawa iterative process for a pair of single-valued and multivalued nonexpansive mappings in Banach spaces. Fixed Point Theory Appl 2010;2010:1–9.
[3] Reich S. Weak convergence theorems for nonexpansive mappings in Banach spaces. J Math Anal Appl 1979;67(2):274–6.
[4] Sahu DR. Applications of the S-iteration process to constrained minimization problems and split feasibility problems. Fixed Point Theory Appl 2011;12(1):187–204.
[5] Maingé PE. Convergence theorems for inertial KM-type algorithms. J Comput Appl Math 2008;219(1):223–36.
[6] Fan, K. A minimax inequality and applications. o shisha ed inequalities III. San Diego: Academic Press; 1972, p. 103–13.
[7] Moudafi A. Split monotone variational inclusions. J Optim Theory Appl 2011;150:275–83.
[8] Li J. Split equilibrium problems for related games and applications to economic theory. Optim 2019;68(6):1203–22.
[9] Suleiman YI, Rehman HUr, Gibali A, Kumam P. A self-adaptive extragradient-CQ method for a class of bilevel split equilibrium problem with application to Nash cournot oligopolistic electricity market models. Comput Appl Math 2020;39(4):293.
[10] Abass HA, Oyewole OK, Narain OK, Jolaoso LO, Olajuwon BI. On split generalized equilibrium and fixed point problems with multiple output sets in real Banach spaces. Comput Appl Math 2022;41(8):416.
[11] Mekruksavanich S, Kaewyong N, Jitpattanakul A, Sitthithakerngkiet K. Adapting step size algorithms for solving split equilibrium problems with applications to signal recovery. J Inequal Appl 2022;2022(1):125.
[12] Kazmi KR, Rizvi SH. Iterative approximation of a common solution of a split equilibrium problem, a variational inequality problem and a fixed point problem. J Egyptian Math Soc 2013;21(1):44–51.
[13] Suantai S, Cholamjiak P, Cho YJ, Cholamjiak W. On solving split equilibrium problems and fixed point problems of nonspreading multi-valued mappings in Hilbert spaces. Fixed Point Theory Appl 2016;2016:1–16.
[14] Ofoedu EU. Strong convergence theorem for uniformly L-Lipschitzian asymptotically pseudocontractive mapping in real Banach space. J Math Anal Appl 2006;321(2):722–8.
[15] Goebel K. Topics in metric fixed point theory. cambridge studies in advanced mathematics/. vol. 28, Cambridge University Press; 1990.
[16] Opial Z. Weak convergence of the sequence of successive approximations for nonexpansive mappings. 1967.
[17] Blum E. From optimization and variational inequalities to equilibrium problems. Math Student 1994;63:123–45.
[18] Combettes PL, Hirstoaga SA. Equilibrium programming in Hilbert spaces. J Nonlinear Convex Anal 2005;6(1):117–36.
[19] Byrne C, Censor Y, Gibali A, Reich S. The split common null point problem. J Nonlinear Convex Anal 2012;13(4):759–75.
[20] Combettes, P L. The convex feasibility problem in image recovery. In: Advances in imaging and electron physics. vol. 95, Elsevier; 1996, p. 155–270.
[21] Huang GB, Zhu QY, Siew CK. Extreme learning machine: theory and applications. Neurocomputing 2006;70(1–3):489–501.
[22] Censor Y, Elfving T. A multiprojection algorithm using bregman projections in a product space. Numer Algorithms 1994;8:221–39.
[23] Thomas T, Pradhan N, Dhaka VS. Comparative analysis to predict breast cancer using machine learning algorithms: a survey. In: 2020 international conference on inventive computation technologies. ICICT, IEEE; 2020, p. 192–6.